CANCER

# Minimal dosing of leukocyte targeting TRAIL decreases triple-negative breast cancer metastasis following tumor resection

Nidhi Jyotsana[1], Zhenjiang Zhang[1], Lauren E. Himmel[2], Fang Yu[1], Michael R. King[1]*



**Surgical removal of primary tumor is a common practice in breast cancer treatment. However, postsurgical metastasis poses an immense setback in cancer therapy. Considering that 90% of cancer-related deaths are due to metastasis, antimetastatic therapeutic strategies that can target disseminating tumor cells in the circulation before they can form secondary tumors hold preclinical and clinical potential for cancer patients. Our current work uses a liposomal formulation functionalized with the adhesion receptor E-selectin and the apoptosis-inducing ligand TNF (tumor necrosis factor)–related apoptosis-inducing ligand (TRAIL) to reduce metastasis following tumor resection in an aggressive triple-negative breast cancer (TNBC) mouse model. We demonstrate that minimal administration of E-selectin–TRAIL liposomes can target metastasis in a TNBC model, with primary tumor resection to mimic clinical settings. Our study indicates that TRAIL liposomes, alone or in combination with existing clinically approved therapies, may neutralize distant metastasis of a broad range of tumor types systemically.**

## INTRODUCTION

Metastasis remains the most critical condition limiting cancer patient survival, and the development of effective treatments against metastatic cancers, especially triple-negative breast cancer (TNBC), is among the greatest challenges in current experimental and clinical cancer research (*1*). Breast cancer represents the most common cancer in women worldwide, and the 5-year survival rate for stage IV female breast cancer cases diagnosed from 2007 to 2013 is 26.5% (*2*). From a clinical perspective, TNBC is a highly relevant subgroup, as these patients do not benefit from endocrine or anti-HER2 (human epidermal growth factor receptor 2) therapy and chemotherapy remains the only therapeutic option.

While surgical removal of breast cancerous tissue may be beneficial, several experimental studies demonstrate that surgical intervention itself generates a permissive environment for accelerated tumor relapse and metastatic growth (*3*). This could be due to the shedding of cancer cells into the circulation and/or a wound healing process that involves local and systemic inflammatory responses (*4*). In experimental animal models of breast cancer, an increase in the number of disseminating cancer cells in circulation is reportedly shown after surgery (*4*). Thus, it is evident that the common practice of surgical resection to eliminate breast tumors could actually serve to advance metastasis. This disease progression via metastasis is often unresponsive to existing therapies and demand novel targeting strategies.

For metastasis to take place, circulating tumor cells (CTCs) detach from the primary breast tumor tissue, enter the blood circulation, extravasate into secondary sites in a selectin-dependent manner, and proliferate there (*5*). The presence of CTCs in the blood serves as a metastasis indicator, and targeting them before they may form secondary tumors holds great therapeutic potential (*6*, *7*). However, the relative rarity of CTCs and lack of identifiable unique markers pose a great challenge in their targeting (*8*).

TNF (tumor necrosis factor)–related apoptosis-inducing ligand (TRAIL), also known as Apo-2 ligand, binds to death receptors 4 and 5 to cause activation of extrinsic caspase-dependent apoptosis signaling (*9*). Several preclinical and clinical studies have used TRAIL as an antitumor therapeutic because it can selectively induce apoptosis in cancer cells while sparing normal cells (*9*–*12*). However, the unstable nature of the soluble form of the protein under physiological conditions, intrinsic or developed TRAIL resistance in many cell lines as well as in primary cancer cells, and hepatotoxicity caused by systemic administration have led to unfavorable clinical trials (*13*, *14*). Various approaches to increasing TRAIL availability and cross-linking efficiency have been explored, along with the use of nanoparticles as TRAIL delivery carriers for improved delivery, better pharmacokinetics, and bioavailability.

Binding of E-selectin–TRAIL liposomes (ETL) to leukocytes and their delivery in vivo to cancer cells in the circulation have been successfully demonstrated (*11*). Selectins facilitate rapid, force-dependent adhesion to selectin ligands on tumor cells and leukocytes in blood; thus, following systemic administration in vivo, our bispecific liposomes adhere to leukocytes to avoid renal clearance and thus increase liposome circulation and bioavailability (*11*, *15*).

Preclinical models with spontaneous metastasis are the gold standard for the development of antimetastatic therapeutics. The 4T1 breast carcinoma is an extremely aggressive TNBC mouse model that is highly tumorigenic and metastatic (*16*, *17*). 4T1 cells injected orthotopically in mammary gland metastasize spontaneously from the primary tumor to distant sites, including the lungs, lymph nodes, liver, brain, and bone, unlike many other tumor models (*16*). Considering the aggressive nature of the cells and onset of metastasis within 2 weeks, the 4T1 breast carcinoma model is viewed as a challenging model for therapeutic targeting, and administration of therapeutics in conjunction with primary tumor resection mimics the clinical setting.

In the present study, we address the problem of postsurgical metastasis by asking whether minimal ETL administration can inhibit tumor metastasis and increase survival of TNBC in preclinical settings. By using bispecific ETL, we show an enhanced therapeutic effect of liposomal TRAIL versus soluble TRAIL on 4T1 cancer cells under

[1]Department of Biomedical Engineering, Vanderbilt University, Nashville, TN 37235, USA. [2]Department of Pathology, Microbiology and Immunology, Translational Pathology Shared Resource, Vanderbilt University Medical Center, Nashville, TN 37232-258, USA.
*Corresponding author. Email: mike.king@vanderbilt.edu

fluid shear stress conditions in vitro, followed by an in vivo proof of concept that minimal administration of ETL can effectively neutralize metastasis in the 4T1 metastatic breast carcinoma model, with resection of the tumor to mimic clinical intervention. By minimizing the surgically induced CTC burst that occurs through minimally invasive surgical techniques (*18*) and by targeting CTCs perioperatively, the intent is to decrease the occurrence of metastasis and achieve improved patient outcomes.

## RESULTS

### 4T1 cells respond to liposomal TRAIL more efficiently than soluble TRAIL

To investigate the apoptotic activity of TRAIL on 4T1 breast cancer cells in vitro and in vivo, we prepared empty or naked liposomes (NL) and ETL formulations (Fig. 1A). A thin lipid film was formed by drying lipids in chloroform. Lipids were then hydrated and subjected to freeze-thaw cycles to form multilamellar liposomes, which were then extruded through membranes to form unilamellar liposomes. A combination of E-selectin and TRAIL was then conjugated to Ni-NTA (nitrilotriacetic acid) on the liposome surface. NL and ETL formulations were analyzed for size and charge characteristics with the Malvern Nano ZS Zetasizer. The liposome size was measured to be 109.1 ± 11 and 120.3 ± 14 nm, respectively, before and after conjugation with TRAIL and E-selectin. Liposome size increase after conjugation is consistent with successful conjugation (Fig. 1B). To test and compare the efficacy of the free soluble form of TRAIL (ST) versus liposomal form (ETL) on 4T1 cancer cells under static culture conditions, we treated 4T1 cells with ST, NL, and ETL at various TRAIL concentrations (100, 200, and 300 ng/ml) for 24 hours under normal cell culture conditions [RPMI growth medium supplemented with 10% fetal bovine serum (FBS) and 1% penicillin/streptomycin at 37°C, 5% $CO_2$]. We observed a dose-dependent decrease in cell viability of 4T1 cells for both ST and ETL (fig. S1). ETL treatment at a higher dose of TRAIL (300 ng/ml) to $1 \times 10^5$ 4T1 cells/ml for 24 hours showed up to a 2.5-fold decrease in cell viability compared to ST and NL (Fig. 1C). These results suggest that a higher dose of TRAIL is required to target 4T1 cells and that 4T1 cells respond more efficiently to ETL compared to ST. Hence, liposomal TRAIL therapy can be used to target highly aggressive triple-negative 4T1 breast carcinoma cells in vitro.

### Piperlongumine, curcumin, and aspirin do not synergize with TRAIL against 4T1 cells

Our observation that a higher dose of ETL therapy is required for killing 4T1 cells encouraged us to investigate whether combination treatment along with TRAIL therapy could be efficacious for the treatment of 4T1 cells in vitro. Piperlongumine (PL), a small-molecule drug known to increase reactive oxygen species levels in cancer cells, has been previously shown to synergize with TRAIL liposomal therapy against prostate and colon cancer cells in vitro and in vivo (*19*). A synergistic antitumor effect of curcumin (Cur) and TRAIL via induced up-regulation of death receptors has also been recently shown in colon cancer cells (*20*). Pretreatment of COLO205 colon cancer cells with 1 mM aspirin (ASP) was shown to significantly sensitize cells to TRAIL-mediated apoptosis (*21*). To study the synergistic effects of PL, Cur, and ASP with TRAIL, we treated 4T1 cells with PL (10 and 20 μM), Cur (10 and 20 μM), and ASP (1 mM) alone or in combination with ST, NL, or ETL (300 ng/ml of TRAIL concentration) under static cell culture conditions for 24 hours, followed by assessment of cell viability. We did not observe any significant increase in apoptosis or decrease in cell viability of 4T1 cells when treated alone or in combination with different concentrations of PL, Cur, and ASP (fig. S2, A to I). Hence, our results demonstrate that combination treatment with PL, Cur, or ASP does not sensitize 4T1 cells to TRAIL therapy in vitro.

### Fluid shear stress sensitizes 4T1 cells to TRAIL-induced apoptosis in vitro

Disseminated tumor cells are exposed to fluid shear stress in the blood circulation (*22*, *23*). By performing in vitro blood spike experiments under shear flow conditions, previous studies from our group indicate that cancer cells can be sensitized to TRAIL treatment (*11*). To investigate the effect of TRAIL treatment on circulating

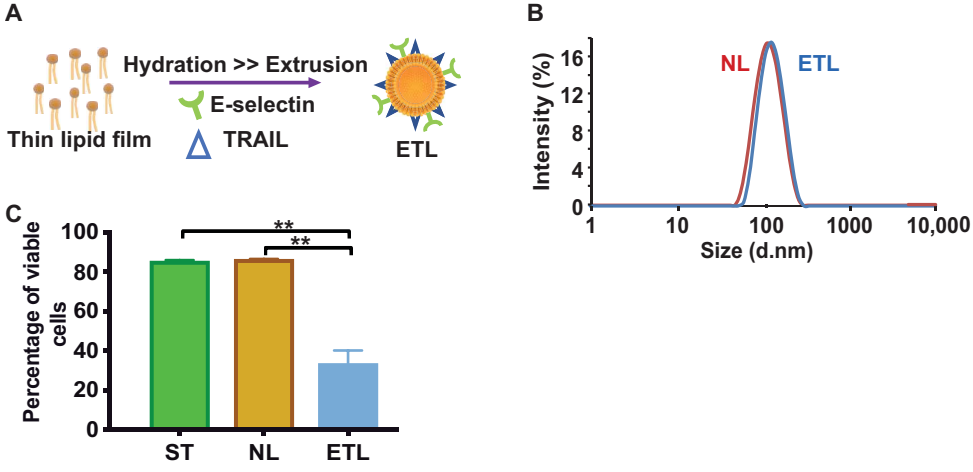


**Fig. 1. ETL kills 4T1 breast carcinoma cells more efficiently than ST under static conditions.** (**A**) ETL formulation schematics. (**B**) Size distribution analysis of ETL formulation using a Zetasizer. (**C**) To assess the ability of ETL to target and kill 4T1 cancer cells under static cell culture conditions, 300 ng of TRAIL per milliliter of ETL was added to $1 \times 10^5$ 4T1 cells/ml for 24 hours. Cells were then washed and assessed for their viability. Percentage of annexin V and propidium iodide (PI) double-negative 4T1 cells after 24 hours of ST, NL, or ETL treatment at 300 ng/ml TRAIL concentration is plotted (mean ± SEM; $n = 3$). $^{**}P < 0.005$.

4T1 breast carcinoma cells under fluid shear stress and in the presence of human blood, we spiked $5 \times 10^5$ 4T1 cells labeled with CellTracker dye into 0.5 ml of whole blood and treated them with ST, NL, or ETL (300 ng/ml of TRAIL concentration) following exposure to shear flow in a cone-and-plate viscometer at a shear rate of 150 $s^{-1}$ for 2 hours. Buffy coat containing 4T1 cells was isolated from whole blood by Ficoll density centrifugation for annexin V/propidium iodide (PI) staining followed by flow cytometry analysis. We observed a significant decrease in viability of ETL-treated 4T1 cells following exposure to shear flow (Fig. 2, A and B). 4T1 breast carcinoma cells

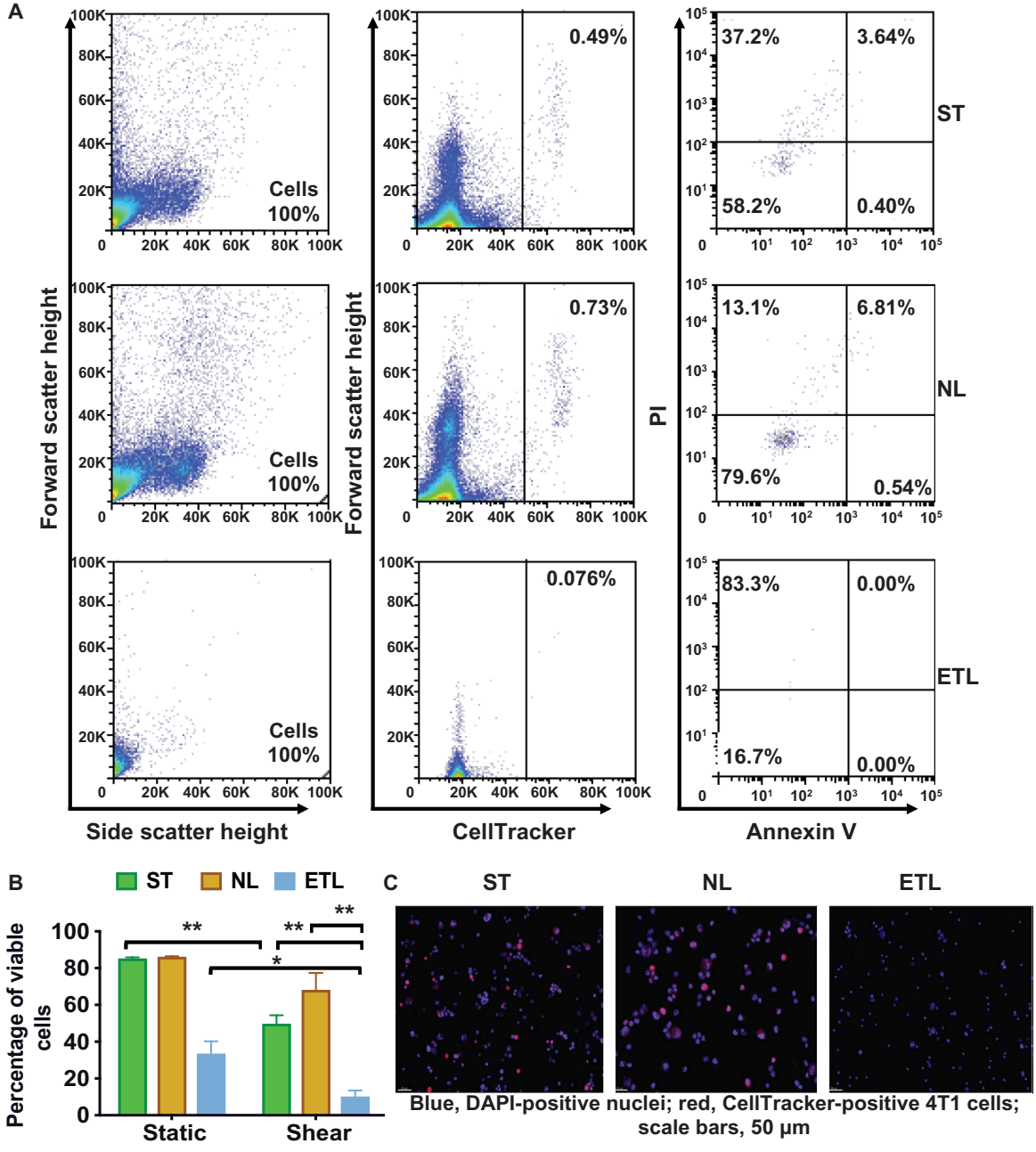


**Fig. 2. Fluid shear stress significantly increases TRAIL-induced 4T1 breast carcinoma cell death in vitro.** 4T1 breast cancer cells ($5 \times 10^5$) labeled with CellTracker dye were spiked into 0.5 ml of whole blood and treated with ST, NL or, ETL (300 ng/ml of TRAIL per milliliter) following exposure to shear flow in a cone-and-plate viscometer, at a shear rate of 150 $s^{-1}$for 2 hours. Buffy coat containing 4T1 cells was isolated from whole blood by Ficoll density centrifugation, washed, and resuspended in calcium-saturated phosphate-buffered saline (PBS). (**A**) Representative annexin V/PI fluorescence-activated cell sorting (FACS) plots of 4T1 cancer cells sheared with ST, NL, or ETL (300 ng of TRAIL per milliliter) after 2 hours. The ETL-treated samples showed a marked loss of intact CellTracker-positive cancer cells, contributing to the notable reduction in cell numbers included in the analysis. (**B**) Percentage of annexin V and PI double-negative 4T1 cells after treatment with ST, NL, or ETL at a TRAIL concentration of 300 ng/ml under static (for 24 hours) or shear flow (2 hours) conditions (mean ± SEM; $n = 3$). (**C**) Representative micrographs of cells in the isolated buffy coat after treatment with ST, NL, or ETL at a TRAIL concentration of 300 ng/ml under shear flow for 2 hours [blue represents 4′,6-diamidino-2-phenylindole (DAPI)/nucleus; red represents 4T1 cells marked with CellTracker dye; scale bars, 50 μm]. *$P < 0.05$ and **$P < 0.005$.

treated with ST, NL, and ETL showed 1.7-, 1.2-, and 3.3-fold decrease in cell viability, respectively, under shear flow conditions (Fig. 2B). In addition, the microscopic examination of the isolated buffy coat displayed 87 and 86% of CellTracker-positive 4T1 cells with normal morphology when treated with ST and NL, respectively, whereas only 46% CellTracker-positive 4T1 cells with clearly disintegrated cellular appearance was observed in the ETL treatment group (Fig. 2C). These results suggest that ETL therapy is more effective in targeting 4T1 cells under blood flow conditions, consistent with previous findings for colorectal and prostate cancer cells from our group (*11*).

### Minimal ETL therapy decreases metastatic burden and extends survival in a 4T1 metastatic TNBC model following tumor resection

To address whether minimal ETL administration can inhibit tumor metastasis, we assessed the efficacy potential of ETL in vivo in the 4T1 breast carcinoma model, with a focus on neutralizing metastasis in conjunction with surgical removal of the primary breast tumor. We injected 30,000 4T1-luc cells (stably expressing luciferase gene) into the fourth mammary fat pad of 8-week-old female BALB/c mice at day 0. The mice were continuously monitored for tumor development via bioluminescence imaging (BLI), followed by "minimal" treatment consisting of three injections (one intraperitoneal injection at day 19 and two intravenous injections at days 17 and 22) of ST, NL, or ETL (2.5 mg/kg TRAIL per injection) in conjunction with surgical removal of the primary tumor (Fig. 3A). Considering the aggressive and invasive nature of the 4T1 breast cancer model, we combined the primary tumor removal surgery with a localized intraperitoneal injection of our formulations (NL/ETL) in the vicinity of the tumor resection site to avoid any further spread of remaining cancer cells spared from surgery into nearby lymph nodes. As there is growing evidence that surgery and intraoperative radiotherapy are efficient treatments for local control, we substituted the intraoperative radiotherapy with localized injection of our formulations in the vicinity of the primary tumor site intraoperatively. This also aided in keeping our treatment regimen minimal and preventing tumor recurrence at the primary tumor site. All of the mice ($n = 28$) injected with 4T1-luc cells developed orthotopic breast tumors that were surgically removed on day 19 (fig. S3A). The mice were divided into three groups ($n = 8$ for ST, $n = 10$ each for NL and ETL) such that their average BLI levels remained uniform (fig. S3B). The primary orthotopic breast tumors were isolated following 48 hours of the first ST, NL, or ETL systemic injection in mice and were evenly bisected perpendicular to the skin surface to enable monitoring of their histology. We observed that necrotic area/tumor area ratio was significantly higher in the ST group compared to the NL group, with no significant differences to the ETL group. Primary tumors in the ETL group were smaller in size with more central necrosis, whereas tumors from the NL treatment group were comparatively bigger with less central necrotic area (Fig. 3, B and C). This suggests that even a single systemic administration of ST or ETL had a beneficial effect by reducing the growth and viability of the 4T1 primary tumors. The metastatic tumor burden in the mice was monitored and quantified using BLI to detect the luciferase signal of 4T1 cells (both at the primary tumor site and disseminated via circulation to secondary organs) following the minimal administration of ST, NL, or ETL. A significant reduction in the metastatic burden was found in the ETL treatment group compared to the NL group with respect to the overall luciferase signal intensity and the number of luciferase signals 1 week after the final ETL administration. While we did not observe a significant difference in the luciferase signal intensity between the ST and ETL groups, the number and intensity of luciferase signals in the ST group was higher than that in the ETL group (Fig. 3, D and E). No reduction in body weight was observed between NL- and ETL-treated mice during the time course of the in vivo study, indicating that mice did not experience any significant adverse effects in relation to surgical removal of the primary tumors and also that the liposomal formulations did not introduce significant toxicity issues in vivo (Fig. 3F). Notably, mice treated with ETL survived significantly longer compared to ST- or NL-treated mice (median overall survival: ETL, 51 days; ST, 45 days; NL, 40 days; Fig. 3G). Two of the ETL group mice are still surviving at the time of this writing with no signs of metastasis or sickness (250 days). The 4T1 mammary carcinoma model closely mimics human mammary cancer, as it is highly invasive and can spontaneously metastasize in as soon as 2 weeks after inoculation of the primary tumor, to multiple distant sites including lung, liver, bone, and lymph nodes (*16*). Hematoxylin and eosin (H&E) staining of the lungs from the moribund mice revealed that all lungs were extensively infiltrated with metastases such that the gross lobar structure was obscured irrespective of the treatment group (ST, NL, or ETL). Pulmonary tissue in all animals was extensively involved in metastatic disease, predominantly in the subpleural location. In addition, vascular space invasion was frequently observed along with areas of pulmonary parenchymal infarction and hemorrhage (Fig. 3H). In many cases, there was so much metastatic tumor present compared to lung tissue that it was difficult to determine whether the lung or adjacent structures (e.g., lymph nodes) were the source of the tumor in some foci. The specimens were so infiltrated that discerning meaningful differences between the treatment groups was not feasible. Despite the presence of advanced pulmonary metastasis, hepatic metastasis was not very evident in this 4T1 metastatic model, as metastatic foci were identified in some of the mice, with no correlation with group (5 of 46 liver lobes analyzed). There was extensive extramedullary hematopoiesis, particularly myeloid lineage, which could possibly obscure tumor micrometastasis (Fig. 3H). In accordance with previous literature, we also observed enlarged spleens/splenomegaly in our 4T1 metastatic breast cancer mice, irrespective of the treatment group. Infiltration of metastatic tumor cells was also observed in bone marrow sections of the evaluated mice (Fig. 3I). All mice, other than the two surviving ETL mice, were eventually euthanized for humane considerations or died because of extensive metastatic burden. Our in vivo efficacy study suggests that minimal ETL therapy has antitumor and antimetastatic effects in the 4T1 postsurgical metastatic breast cancer model that leads to improved survival.

### ETL treatment reduces the number of disseminating 4T1 metastatic cells in mouse circulation

To test the ability of ETL to target metastatic cancer cells within the circulation of mice, we injected 30,000 4T1 cells stably expressing mCherry protein (4T1-mCherry) into the mammary fat pad of 12-week-old BALB/c mice. These mice were divided into three groups ($n = 4$ for each group) on day 16 based on their tumor size. Mice were injected with ST, NL, or ETL (each injection with 2.5 mg/kg TRAIL dose) in an administration profile identical to our in vivo efficacy study (three injections; one intravenous on day 17, one intraperitoneal on day 19, and one intravenous on day 22) (Fig. 3A). Tail bleeding was performed at days 15, 20, and 25 to collect peripheral blood from mice. The presence of disseminating cancer cells in the

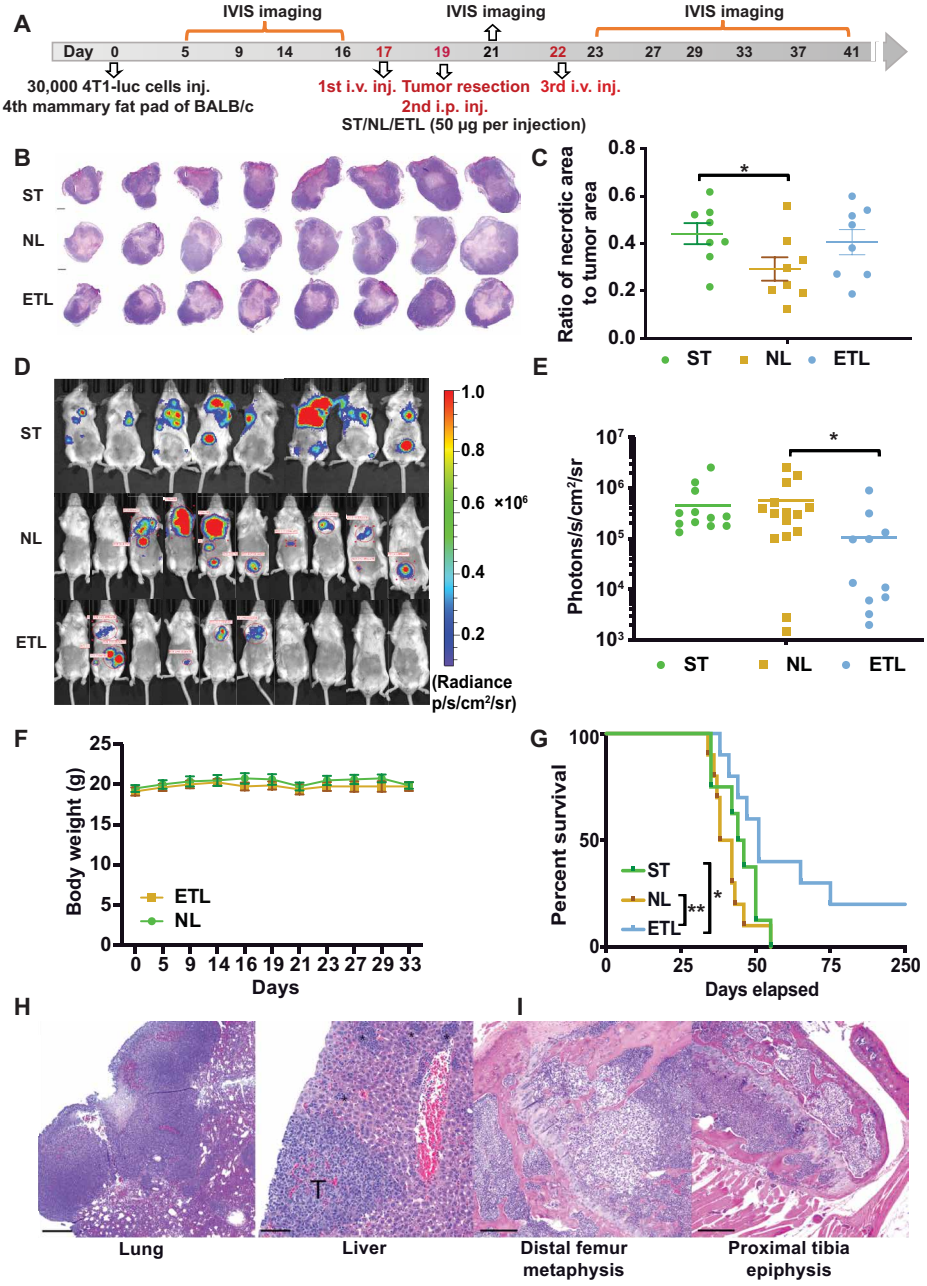


**Fig. 3. Minimal treatment of ETL decreases metastatic burden and prolongs survival in the 4T1 breast carcinoma model after tumor resection.** (**A**) Timeline of in vivo experiment. i.v., intravenous; i.p., intraperitoneal. (**B**) Photomicrographs (H&E stain) of the isolated primary tumors taken (scale bars, 1 mm) to show the tumor size and central necrosis in ST-, NL-, and ETL-treated mice followed by (**C**) graphical representation of the ratio of necrotic area to tumor area after digitization and image analysis. (**D**) Antimetastatic effect of ETL in vivo, as shown by IVIS imaging of bioluminescence in 4T1 metastatic breast carcinoma mice that received mammary fat pad transplant of 4T1-luc cells (4T1 cells stably expressing luciferase) and were treated with three injections of ST, NL, or ETL (50 µg per injection; before, during, and after tumor resection within a period of 6 days; $n = 10$). IVIS imaging was performed at day 13 and day 8 after the first and last injections, respectively. Graphical representation of quantitation of IVIS imaging of (**E**) overall luciferase signal. (**F**) Mouse body weight during the course of the in vivo study at indicated time points (Fig. 4A; mean ± SEM; $n = 10$). (**G**) Survival of 4T1 metastatic breast carcinoma mice that received mammary fat pad transplant of 4T1-luc cells and were treated with three injections of ST, NL, or ETL (50 µg per injection), designating the transplantation date as day 0 ($n = 10$). (**H**) Photomicrographs of the lung (scale bar, 500 µm) and liver (scale bar, 100 µm) to show metastatic foci in NL and ETL treatment groups, respectively, with a focus of vascular space invasion in lung compared to the small metastatic foci in the liver (T) with extramedullary hematopoiesis (asterisks). (**I**) Photomicrographs of distal femur and proximal tibia (scale bars, 250 µm) to show bone metastasis. *$P < 0.05$ and **$P < 0.005$.

mouse circulation was monitored by quantifying the percentage of 4T1-mCherry–positive cells in peripheral blood using flow cytometry (Fig. 4A). We also checked for the presence of mCherry–positive cancer cells in the peripheral blood via confocal imaging (Fig. 4B). Similar to previous literature findings, we observed a substantial overall increase in the percentage of 4T1-mCherry cells in the peripheral blood immediately after tumor resection (day 20), which decreased at a later time (day 25), irrespective of the treatment

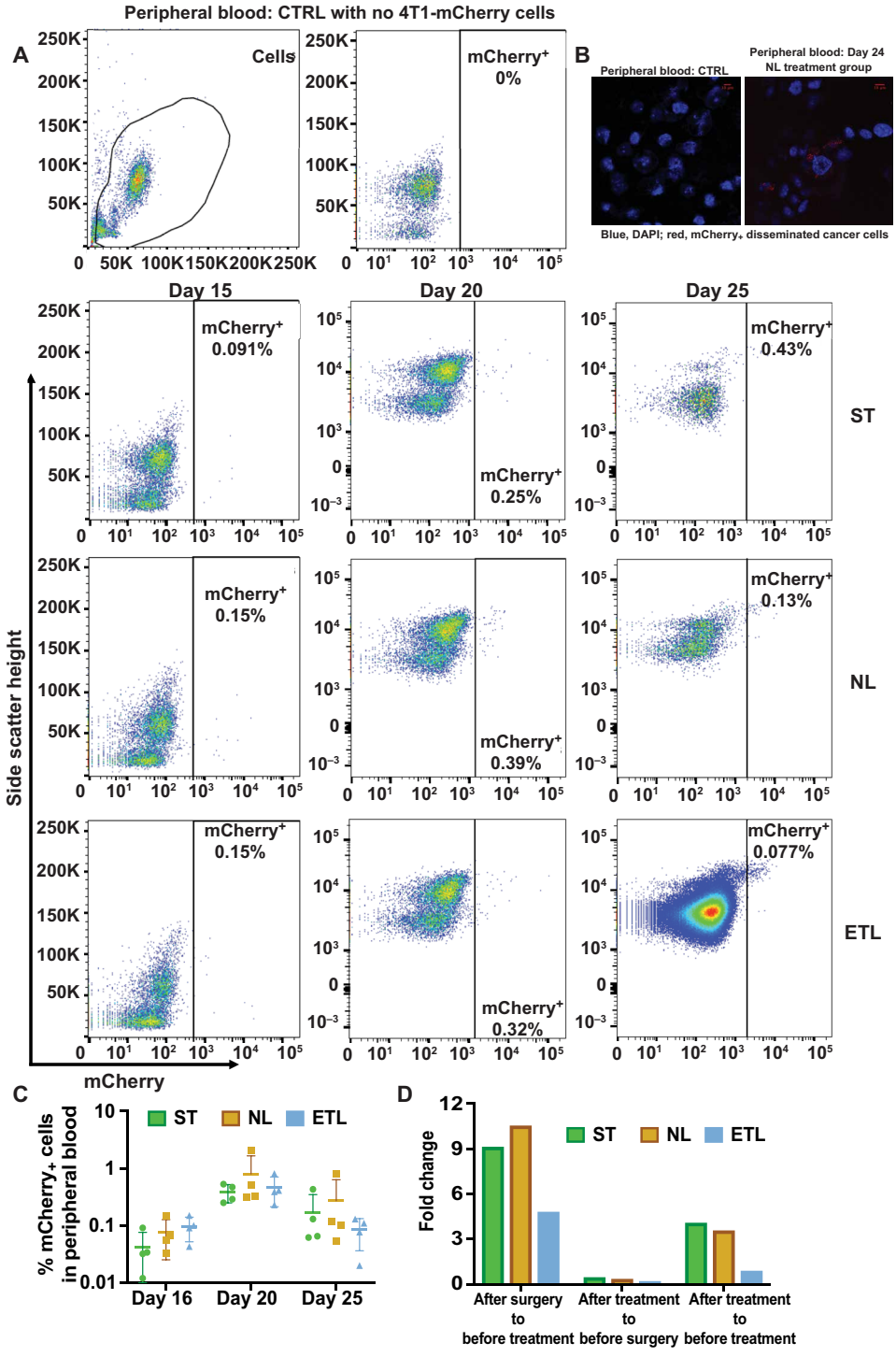


**Fig. 4. ETL treatment reduces disseminated 4T1 metastatic cells in circulation in vivo.** To investigate whether ETL treatment can target metastatic cancer cells flowing in the circulation of mice, 30,000 4T1-mCherry cells were injected in the fourth mammary fat pad of 12-week-old healthy BALB/c mice ($n = 4$ per group) followed by treatment with three injections of ST, NL, or ETL (50-μg TRAIL dose). The time and mode of injections were identical to those specified for Fig. 3A. Tail bleeding was performed at day 15 (before treatment), day 20 (after surgery and two injections), and day 25 (after treatment) to collect peripheral blood from mice. (**A**) Representative FACS plots of peripheral blood cells from the ST, NL, or ETL treatment group at different time points. The presence of disseminating cancer cells in mouse circulation is shown by mCherry-positive cells in the plots. (**B**) Representative micrographs of cells in the isolated peripheral blood at day 20 from mice with 30,000 cells injected in the fourth mammary fat pad at day 0 (blue represents DAPI/nucleus; red represents mCherry-positive disseminated cancer cells). (**C**) Graphical representation of quantitation of 4T1-mCherry–positive cells in peripheral blood using flow cytometry in the ST, NL, or ETL treatment group ($n = 4$) at different time points. (**D**) Graphical representation of fold change in the percentage of mCherry-positive cancer cells in the circulation in the ST, NL, or ETL treatment group ($n = 4$) at different time points.

group (Fig. 4, A and C). A twofold reduction in mCherry-positive cells was observed in the ETL treatment group versus ST and NL groups following surgery (day 20 and two injections of ST, NL, or ETL) and again, following three injections of ST, NL, or ETL (Fig. 4D). Notably, an increase of 4-, 3.55-, and 0.88-fold in mCherry-positive disseminating cancer cells was observed in ST, NL, and ETL treatment groups, respectively, before and after treatment (Fig. 4D). The physical binding of ETL on leukocytes and a reduction in the viability of circulating cancer cells has been previously demonstrated by our group (*11*). Accordingly, our results show a reduction in metastasis burden of disseminated breast cancer cells in the circulation by ETL treatment.

### Minimal administration of ETL is safe and demonstrates good tolerability in mice

Next, we investigated the safety profile of ETL administration in vivo. Healthy BALB/c mice (12 weeks old) were injected with phosphate-buffered saline (PBS) (CTRL) or ETL in an administration profile identical to our in vivo efficacy study (three injections; one intraperitoneal and two intravenous within a time period of 6 days) (Fig. 3A). No reduction in total body weight and relative organ weight of ETL mice was observed compared to CTRL mice (Fig. 5, A to C). However, a significant increase in relative spleen weight was observed in mice treated with ETL compared to CTRL mice (Fig. 5C). Examination of complete blood counts of ETL-treated

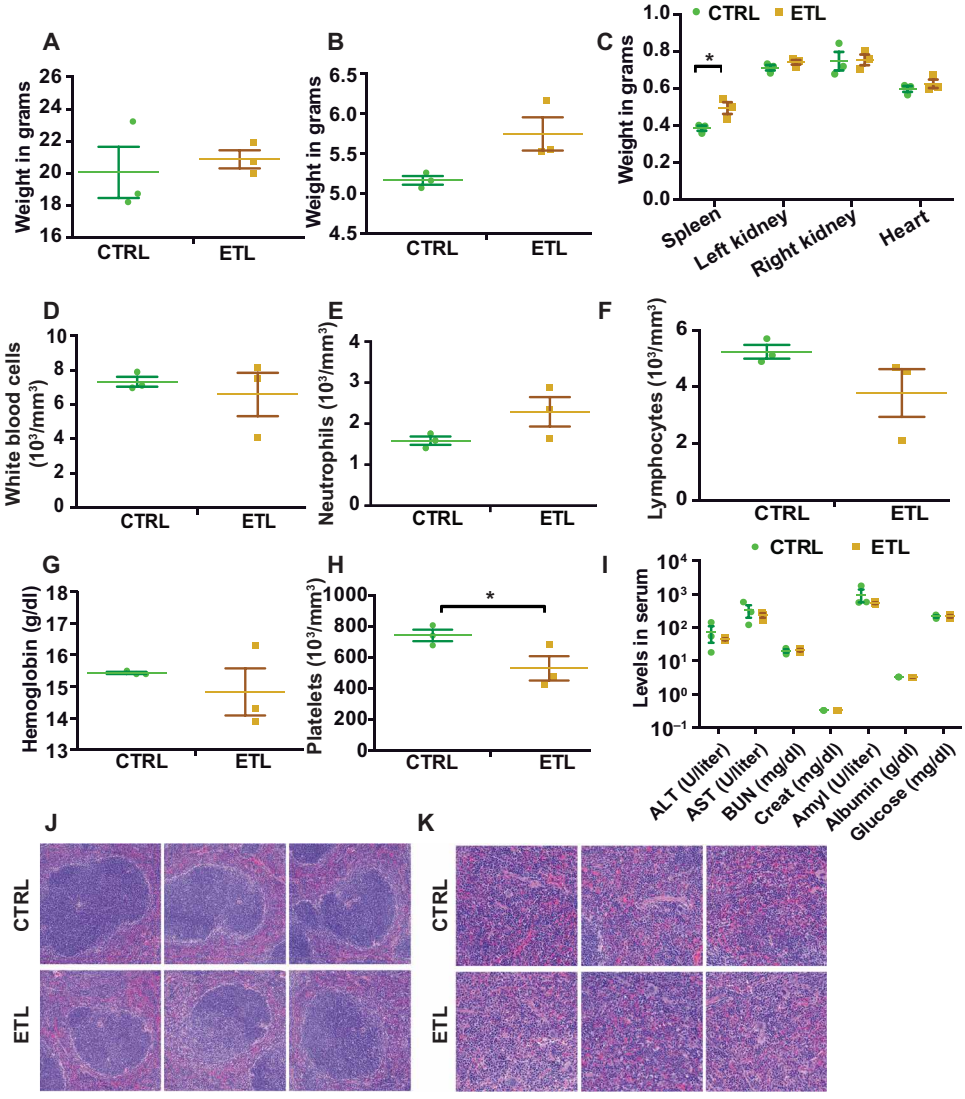


**Fig. 5. Minimal administration of ETL is tolerable and safe in mice.** To monitor the safety profile of ETL administration in mice, 12-week-old healthy BALB/c mice ($n = 3$ per group) were treated with three injections of PBS/CTRL or 50 μg of ETL. The time and mode of injections were identical to those specified for Fig. 3A. The mice were monitored and euthanized 24 hours after the final injection for the following analysis: (**A**) total mouse body weight, (**B**) relative liver weight, (**C**) relative organ weight (spleen, kidney, and heart), (**D**) white blood cell count, (**E**) total neutrophil count, (**F**) total lymphocyte count, (**G**) hemoglobin levels, and (**H**) platelet count in peripheral blood of mice (mean ± SEM; $n = 3$). (**I**) Serum biochemical profile in mice (serum was collected at 24 hours following the last injection; ALT, alanine aminotransferase; Creat, creatinine; BUN, blood urea nitrogen; AST, aspartate aminotransferase; Amyl, amylase; mean ± SEM; $n = 3$). Representative photomicrographs of spleen histology sections of (**J**) the splenic white pulp area and (**K**) the splenic red pulp area from the mice ($n = 3$). *$P < 0.05$.

mice revealed no significant differences in number of leukocytes, with neutrophils, lymphocytes, and hemoglobin, compared to PBS-treated mice (Fig. 5, D to G). However, a significant decrease in the number of platelets was found in the peripheral blood of ETL-treated mice (Fig. 5H); these values are within the previously reported normal range (515 to 1150 × $10^3$/$mm^3$) of platelet counts in female BALB/c mice (*24*, *25*). Serum analysis showed no significant toxicity in mice following administration of ETL (Fig. 5I). No liver toxicity was found, as there were no significant differences in the levels of liver enzymes such as alanine aminotransferase and aspartate aminotransferase. Comparable levels of urea (blood urea nitrogen) and creatinine between PBS/ETL-treated mice suggests that the kidney function was normal. Normal levels of amylase enzyme indicate no pancreatic toxicity. Levels of albumin and glucose in the serum were similar in PBS/ETL-treated mice. In the splenic white pulp (periarteriolar lymphoid sheaths), we observed mild lymphoid hyperplasia in ETL-treated animals compared to CTRL, as evidenced by activating germinal centers, polarity, and increased mitoses (Fig. 5J). In addition, in the splenic interfollicular red pulp area, mildly increased extramedullary hematopoiesis in ETL animals was observed compared to CTRL (Fig. 5K). Myeloid and lymphoid hyperplasia typically indicate antigenic stimulation and can partially explain the enlarged spleens in ETL treatment mice. Our in vivo toxicity study thus suggests overall good tolerability of the minimal ETL administration in mice.

## DISCUSSION

Postsurgical metastasis poses an immense setback in cancer therapy, especially in breast cancer. While chemotherapy and surgical removal of tumor tissue may be beneficial, disease progression and relapse via metastatic spread clearly demands effective targeting strategies used in combination. Notably, the side effects associated with standard treatments like chemotherapy and radiotherapy suggest that minimizing the dosage of anticancer therapeutics is highly desirable. TNBC is highly aggressive and metastatic and continues to be an incurable leading cause of mortality especially among women of African American ancestry (*26*). Useful treatments that target progesterone (PR), estrogen (ER), and HER2 are not effective for TNBC, and special treatment approaches are solely needed (*27*).

In this study, we exploited the cancer cell killing activity of TRAIL to answer whether disseminated cancer cells with metastatic potential could be targeted via minimal therapeutic treatment in a TNBC model, with tumor resection. It has been previously shown that E-selectin–targeted liposomes are more effective than empty liposomes in killing cancer cells (*28*). TNBCs have increased concentrations of tumor-infiltrating lymphocytes that have been associated with improved disease-free and overall survival rates in patients (*29*, *30*). Since both leukocytes and disseminated cancer cells adhere to E-selectin in blood (*11*), decorating biocompatible liposomes with recombinant human E-selectin along with TRAIL makes our therapeutic strategy more specific and effective in terms of adhering to leukocytes and cancer cells expressing E-selectin ligands and killing them via reversible TRAIL binding to death receptors. In vitro, ETLs (liposomes functionalized with E-selectin and TRAIL) were significantly more effective in inducing apoptosis in 4T1 cells under static conditions and fluid shear conditions that mimic the circulatory microenvironment. ETLs have been previously shown to adhere to leukocytes in blood under shear conditions in vitro (*11*). Previous attempts to administer ST in vivo have proven ineffective in part because of an extremely short half-life in circulation (*13*). Our in vivo study indicates that, if introduced as a liposomal formulation at appropriate time points, even minimal administration of ETL can serve as a means to neutralize metastasis. Primary tumors in the ETL group were smaller in size with more central necrosis compared to the NL treatment group, suggesting that even a single systemic administration of ETL affects the growth and viability of 4T1 primary tumors. The delay in onset of metastasis and prolonged survival in the longer-term 4T1 metastatic breast cancer model in conjunction with tumor resection addresses the translatability of ETL as an antitumor and antimetastatic therapy into the clinic. This is further supported by a safe and well-tolerable profile of minimal ETL administration in mice.

The unfavorable prognosis and adverse outcomes in TNBC is due to extremely high mutational frequencies, resulting in intratumoral heterogeneity and drug resistance (*29*, *31*). For example, the overexpression of epithelial growth factor receptor (EGFR) in most forms of TNBC increases their resistance to conventional therapies (*32*). EGFR small interfering RNA (siRNA) and anti-EGFR antibody or small-molecule inhibitors targeting EGFR mRNA and protein, respectively, can be delivered via nanoparticles as a combination therapy along these lines (*33*). In addition, BCL-2-like protein 12 (BCL2L12) and superoxide dismutase 1 siRNAs have been recently shown to sensitize breast cancer cell lines MDA-231 and TRAIL-resistant MCF-7 to TRAIL-induced cell death (*34*). Combinatorial approaches using ETL in combination with compounds that have been shown to synergize with TRAIL in various cancer cells (*19*, *21*) may be used to sensitize cancers like 4T1 that show sensitivity to higher doses of TRAIL. Although we did not observe any synergistic effects by combining TRAIL with PL, Cur, and ASP in 4T1 cells, next steps could include combining TRAIL with siRNAs targeting frequently mutated and up-regulated oncoproteins such as VEGF (vascular endothelial growth factor) (*35*) and cellular members of the extrinsic apoptotic pathway such as XIAP (X-linked inhibitor of apoptosis) and c-FLIP [cellular FLICE (Fas-associated death domain protein–like interleukin-1β–converting enzyme)–inhibitory protein]. XIAP has been implicated in TRAIL resistance of many leukemia cell lines, and moreover, its overexpression in tumors is associated with resistance to chemotherapeutic drugs (*36*). Whether its down-regulation can sensitize cells to TRAIL is something that has not yet been determined.

Combination therapies have emerged as a powerful substitute to monotherapy, as they target cancer cells by overcoming multiple resistance mechanisms. Screen-based identification and validation of novel TRAIL sensitizers from Food and Drug Administration–approved drug libraries or libraries of chemotherapeutic drugs, siRNA, peptides, or cytokines could lead to the development of effective combination anticancer therapies (*37*). Poly(adenosine 5′-diphosphate–ribose) polymerase inhibitors, VEGF inhibitors, and phosphatidylinositol 3-kinase/AKT/mammalian target of rapamycin inhibitors are either in or on their way to clinical trials for TNBC treatment (*38*). A study by Liu *et al.* (*39*) demonstrated that blocking Fas signaling in an orthotopic 4T1 mammary carcinoma model significantly reduced tumor growth and metastasis in mice and prolonged survival. Thus, combination therapies with liposomal TRAIL might be helpful for the treatment of patients who are resistant to standard treatments and TRAIL monotherapy.

It has been previously shown that shear stress sensitization response in colon and prostate cancer cell lines is specific to TRAIL-mediated

apoptosis (*40*). Disseminated metastatic cancer cells are exposed to elevated fluid shear forces once they enter the circulation. Thus, shear-induced sensitization to TRAIL in vitro along with significant anti-metastatic behavior in vivo suggests a synergistic response to triple-negative 4T1 breast cancer cells. Moreover, we did not observe any hepatotoxicity effects in vivo after minimal administration of ETL. Since safety has not been a major issue for TRAIL therapy in preclinical and clinical settings, further combinatorial preclinical studies might pave the way toward the use of liposomal TRAIL therapy in TNBC clinical trials.

A major focus of current research involves the development of therapies based on target-specific genetic changes. Although this promises less toxic tailored therapies, the results have been less beneficial than expected primarily because of the molecular heterogeneity within cells from primary tumors and metastases. Moreover, in most patients, by the time of diagnosis, metastasis has already occurred and surgical resection of the primary tumor is not likely curative. None of the existing targeted therapies have yet been evaluated in phase 3 clinical trials, and chemotherapy is still the only validated therapy option for treatment of TNBC in clinical practice. We believe that our current approach represents an important initial step in using targeted ETL to reduce the number of metastatic cancer cells in the bloodstream. Thus, therapeutics like TRAIL alone or in combination could successfully neutralize highly heterogeneous and aggressive metastatic cancers such as TNBC. In summary, the problem of metastasis after surgical resection is really the driving force behind our study, and it supports the potential of minimal administration of liposomal TRAIL to neutralize metastasis in conjunction with surgical resection.

## MATERIALS AND METHODS

### Cell line and cell culture

The breast cancer cell line 4T1 was obtained from the American Type Culture Collection (CRL-2539) and cultured in RPMI 1640 supplemented with 2 mM L-glutamine, 25 mM Hepes, 10% (v/v) FBS, and penicillin/streptomycin (100 U/ml) under humidified conditions at 37°C and 5% $CO_2$. 4T1 cells were seeded in multiwell plates at a seeding density of 100,000 cells/ml 1 day before experimentation to make sure that the cells were in the linear phase of the growth cycle. Cells were treated with 1× Dulbecco's PBS, ST, empty liposomes or NL, and ETLs. The treated cells were maintained in culture conditions for 24 hours and later analyzed by annexin V assay and AlamarBlue assay to quantify the proportion of viable cells.

### Formulation of liposomes

#### *Reagents*

L-α-Lysophosphatidylcholine from egg (Egg PC), sphingomyelin from egg (Egg SM), cholesterol (Chol), and 1,2-dioleoyl-*sn*-glycero-3-[(*N*-(5-amino-1-carboxypentyl)iminodiacetic acid)succinyl] (nickel salt) (DOGS-Ni-NTA), either dissolved in chloroform or in powder form, were purchased from Avanti Polar Lipids. Recombinant human E-selectin Fc chimera protein and TRAIL protein, both with a His-tag, were purchased from R&D Systems and Enzo Life Sciences, respectively.

#### *Preparation of empty and ETLs*

Empty liposomes were made using a lipid film hydration/extrusion method. Briefly, Egg PC, Egg SM, Chol, and DOGS-NTA-Ni were mixed at a molar ratio of 45:30:18:7 in chloroform in a test tube. A lipid film was obtained after removing chloroform completely with overnight vacuum. PBS (1 ml) was added to the test tube to hydrate the lipid film and make multilamellar liposomes. After hydration with occasional vortex for >1 hour, the lipid suspension was then subject to 20 extrusion cycles through 100-nm polycarbonate membrane filters (Nuclepore; Whatman) to produce unilamellar nanoscale liposomes. For protein conjugation, E-selectin and TRAIL proteins were incubated with freshly made liposomes for 30 min at 37°C to allow protein binding via the interaction between His-tag and Ni-NTA. To remove unbound TRAIL and E-selectin, protein conjugated liposomes were purified with high-performance liquid chromatography equipped with a size exclusion chromatography column (60 cm; TSKgel G4000PW; Tosoh Bioscience). Liposome size was measured by dynamic light scattering before and after conjugation (Zetasizer Nano ZS; Malvern Instruments Ltd.)

### Spiking of 4T1 cells into human blood

Peripheral blood was drawn from healthy volunteers after informed consent. 4T1 cells seeded 1 day before each experiment were gently detached from the surface using PBS-based enzyme-free cell detachment solution or Accutase. 4T1 breast cancer cells (500,000) were loaded with 5 μM CellTracker Blue CMAC (7-amino-4-chloromethylcoumarin) by incubating them with the dye in the dark at 37°C. The CMAC-loaded cells were then washed twice using PBS. The pellet was suspended in 0.5 ml of whole blood. Then, 10 μl of PBS, NL, ST, or ETL at 300 ng/ml TRAIL concentration was added to 490 μl of cell suspension in blood (at $10^6$ cells/ml) and immediately added to the cone-and-plate viscometer to simulate the shear-stress conditions of blood flow. Cell suspensions were exposed to shear flow at a shear rate of 150 $s^{-1}$ for 2 hours. All samples were exposed to shear flow at room temperature to prevent potential sample evaporation and/or drying in the cone-and-plate viscometer over prolonged periods of shear. After shearing, the blood sample was collected from the device and carefully layered over 3 ml of Ficoll and centrifuged at 480*g* for 50 min at room temperature. The buffy coat containing mononuclear cells and cancer cells was recovered and washed twice in resuspension buffer, collected, and analyzed for viable fluorescent cancer cells using flow cytometry or stained with 4′,6-diamidino-2-phenylindole and analyzed via confocal microscopy (Zeiss LSM 880).

### Annexin V assay

Quantitation of cell death was analyzed using the annexin V apoptosis assay on a Guava easyCyte flow cytometer (Millipore, Billerica, MA, USA), as previously described (*11*). Samples were prepared per the manufacturer's instructions. Cells were classified into four categories based on dye uptake: viable cells (negative for annexin V and PI), early apoptotic cells (positive for annexin V only), late apoptotic cells (positive for annexin V and PI), and necrotic cells (positive for PI only).

### AlamarBlue assay

AlamarBlue assay for cell viability was performed as previously described (*11*). Ten thousand cells were seeded in 100 μl of media in each well of a 96-well flat bottom transparent plate. One-tenth volume of the AlamarBlue reagent (G-Biosciences, 786-921) was directly added to the wells and incubated for 4 hours at 37°C in a cell culture incubator, protected from direct light. Results were recorded by measuring fluorescence using a fluorescence excitation wavelength with a peak excitation of 570 nm and a peak emission of 585 nm on a microplate reader (Tecan Infinite F500, Tecan Group Ltd.).

### 4T1 mouse model

Mice were housed under specific pathogen–free conditions, and all experimental procedures were approved by the Vanderbilt University Institutional Animal Care and Use Committee and were conducted in an Association for Assessment and Accreditation of Laboratory Animal Care–accredited facility.

#### *4T1 tumor establishment*

Female BALB/cJ mice (8 to 12 weeks old) weighing between 18 and 20 g were obtained from the Jackson Laboratory. Animals were housed at 22 ± 5°C in a 12-hour light/dark cycle and fed rodent chow and water freely. Orthotopic mammary fat pad implantation was performed as follows: 30,000 4T1-luc or 4T1-mCherry cells were injected (50-μl cell suspension in PBS) in the right fourth mammary gland with a 30-gauge needle (BD Biosciences, San Jose, CA, USA), under anesthesia by continuous inhalation of 2% isoflurane gas for 5 to 10 min. Injections were performed under sterile conditions. Bioluminescence images of primary tumor and subsequent metastasis were captured using an IVIS Lumina III imaging system (PerkinElmer Inc.) 5 min after intraperitoneal injection of D-luciferin (150 mg/kg; 100 μl). Mice were euthanized at humane end points.

#### *Tumor resection*

Nineteen days after injection of 4T1 cells, primary tumors were resected. Hairs from the resection site were removed 24 hours before surgery using Nair hair removal cream. Mice were kept under anesthesia during surgery. Mice received subcutaneous injections of ketoprofen (2 mg/kg) immediately before surgery and 24 hours after surgery. The surgical site was cleaned with iodine and ethanol. An incision adjacent to the tumor was made with surgical sharp-blunt–type scissors, and the tumor was gently teased away from the skin with needle-nose forceps and removed. After removal of the tumor, the incision was sutured with 4-0 silk nonabsorbable surgical sutures. Upon completion of the surgery, mice were moved to the recovery area under slightly warm conditions (under a heat lamp). Mice were brought back to the mouse facility after they had resumed consciousness and were monitored every alternate day for labored breathing, metastatic nodules, and primary tumor recurrence.

#### *Treatment*

To test the efficacy of ETL on the progression of metastases, mice were injected with 100 μl of ST, NL, or ETL (50 μg of TRAIL per injection) through the tail vein. Mice were divided into three groups based on intensity of BLI or tumor size on day 16. Mice were given three doses: 48 hours before the tumor is resected (day 19), immediately after the surgery, and 72 hours after the tumor resection. The entire in vivo schematics is shown in Fig. 3A, where the days marked in red indicate the three injection time points.

#### *Hematological and histological evaluation of mice*

Tail bleeding was performed at different time points for quantitation of mCherry-positive disseminated 4T1 cells in peripheral blood. Red blood cell (RBC) lysis was done using RBC lysis buffer for 20 min, and flow cytometry was performed to monitor mCherry-positive cells. Mice were euthanized by $CO_2$ asphyxiation followed by terminal blood collection via cardiac puncture. Body and organ weights were recorded; then, tissues were fixed in 10% neutral buffered formalin immediately following euthanasia of the mice. Complete blood counts were performed on the Forcyte Hematology Analyzer (Oxford Science), and serum chemistry was performed on the ACE Alera (Alfa Wassermann) clinical chemistry analyzer. Spleens were evaluated histologically on the basis of the organ weight data.

Primary tumors were evenly bisected perpendicular to the skin surface, unbiased sectioning of the liver was performed, lungs were embedded whole on the thoracic pluck, and one tibia and one femur were evaluated. Formalin-fixed tissues were routinely processed using a standard 8-hour processing cycle of graded alcohols, xylenes, and paraffin wax, embedded and sectioned at 4 to 5 μm, floated on a water bath, and mounted on hydrophilic glass slides. Bone decalcification was performed using Immunocal (StatLab, McKinney, TX). H&E staining was performed on the Gemini autostainer (Thermo Fisher Scientific, Waltham, MA). All histopathologic interpretation was conducted by a board-certified veterinary pathologist under masked conditions. Photomicrographs were captured on an Olympus BX43 microscope (Olympus Corporation, Tokyo, Japan) equipped with a SPOT Flex camera and software setup (Diagnostic Instruments Inc., Sterling Heights, MI). Quantification of intratumoral necrotic regions was conducted using QuPath, an open-source digital pathology platform.

### Statistical analysis

All experimental data were obtained in triplicate and presented as means ± SEM unless otherwise stated. All graphical error bars represent SEM. Significance was determined by performing an unpaired two-tailed $t$ test with $P < 0.05$ considered significant in GraphPad Prism. Median survival was calculated using Mantel-Cox (log-rank) test in GraphPad Prism.

## SUPPLEMENTARY MATERIALS

Supplementary material for this article is available at http://advances.sciencemag.org/cgi/content/full/5/7/eaaw4197/DC1

Fig. S1. ETL kills 4T1 breast carcinoma cells in a dose-dependent and more efficient manner than ST under static conditions.

Fig. S2. PL, Cur, and ASP do not sensitize 4T1 cells to liposomal TRAIL treatment under static conditions.

Fig. S3. Tumor resection efficiently removes 4T1 primary tumor burden in mice.

## REFERENCES AND NOTES


1. K. A. Cronin, A. J. Lake, S. Scott, R. L. Sherman, A.-M. Noone, N. Howlader, S. J. Henley, R. N. Anderson, A. U. Firth, J. Ma, B. A. Kohler, A. Jemal, Annual report to the nation on the status of cancer, part I: National cancer statistics. *Cancer* **124**, 2785–2800 (2018).
2. R. L. Siegel, K. D. Miller, A. Jemal, Cancer statistics, 2018. *CA Cancer J. Clin.* **68**, 7–30 (2018).
3. S. Tohme, R. L. Simmons, A. Tsung, Surgery for cancer: A trigger for metastases. *Cancer Res.* **77**, 1548–1552 (2017).
4. J. A. Krall, F. Reinhardt, O. A. Mercury, D. R. Pattabiraman, M. W. Brooks, M. Dougan, A. W. Lambert, B. Bierie, H. L. Ploegh, S. K. Dougan, R. A. Weinberg, The systemic response to surgery triggers the outgrowth of distant immune-controlled tumors in mouse models of dormancy. *Sci. Transl. Med.* **10**, eaan3464 (2018).
5. M. Cristofanilli, G. T. Budd, M. J. Ellis, A. Stopeck, J. Matera, M. C. Miller, J. M. Reuben, G. V. Doyle, W. J. Allard, L. W. M. M. Terstappen, D. F. Hayes, Circulating tumor cells, disease progression, and survival in metastatic breast cancer. *N. Engl. J. Med.* **351**, 781–791 (2004).
6. M. Cristofanilli, D. F. Hayes, G. T. Budd, M. J. Ellis, A. Stopeck, J. M. Reuben, G. V. Doyle, J. Matera, W. J. Allard, M. C. Miller, H. A. Fritsche, G. N. Hortobagyi, L. W. M. M. Terstappen, Circulating tumor cells: A novel prognostic factor for newly diagnosed metastatic breast cancer. *J. Clin. Oncol.* **23**, 1420–1430 (2005).
7. S. Riethdorf, H. Fritsche, V. Muller, T. Rau, C. Schindlbeck, B. Rack, W. Janni, C. Coith, K. Beck, F. Janicke, S. Jackson, T. Gornet, M. Cristofanilli, K. Pantel, Detection of circulating tumor cells in peripheral blood of patients with metastatic breast cancer: A validation study of the CellSearch system. *Clin. Cancer Res.* **13**, 920–928 (2007).
8. E. Lin, T. Cao, S. Nagrath, M. R. King, Circulating tumor cells: Diagnostic and therapeutic applications. *Annu. Rev. Biomed. Eng.* **20**, 329–352 (2018).
9. S. Wang, W. S. El-Deiry, TRAIL and apoptosis induction by TNF-family death receptors. *Oncogene* **22**, 8628–8633 (2003).
10. E. C. Wayne, S. Chandrasekaran, M. J. Mitchell, M. F. Chan, R. E. Lee, C. B. Schaffer, M. R. King, TRAIL-coated leukocytes that prevent the bloodborne metastasis of prostate cancer. *J. Control. Release* **223**, 215–223 (2016).

11. M. J. Mitchell, E. Wayne, K. Rana, C. B. Schaffer, M. R. King, TRAIL-coated leukocytes that kill cancer cells in the circulation. *Proc. Natl. Acad. Sci. U.S.A.* **111**, 930–935 (2014).
12. D. W. Stuckey, K. Shah, TRAIL on trial: Preclinical advances in cancer therapy. *Trends Mol. Med.* **19**, 685–694 (2013).
13. S. von Karstedt, A. Montinaro, H. Walczak, Exploring the TRAILs less travelled: TRAIL in cancer biology and therapy. *Nat. Rev. Cancer* **17**, 352–366 (2017).
14. M. Jo, T.-H. Kim, D.-W. Seol, J. E. Esplen, K. Dorko, T. R. Billiar, S. C. Strom, Apoptosis induced in normal human hepatocytes by tumor necrosis factor-related apoptosis-inducing ligand. *Nat. Med.* **6**, 564–567 (2000).
15. P. Gassmann, M.-L. Kang, S. T. Mees, J. Haier, In vivo tumor cell adhesion in the pulmonary microvasculature is exclusively mediated by tumor cell–endothelial cell interaction. *BMC Cancer* **10**, 177 (2010).
16. B. A. Pulaski, S. Ostrand-Rosenberg, Mouse 4T1 breast tumor model. *Curr. Protoc. Immunol.* **39**, 20.2.1–20.2.16 (2000).
17. K. Tao, M. Fang, J. Alroy, G. G. Sahagian, Imagable 4T1 model for the study of late stage breast cancer. *BMC Cancer* **8**, 228 (2008).
18. N. Sawabata, S. Funaki, T. Hyakutake, Y. Shintani, A. Fujiwara, M. Okumura, Perioperative circulating tumor cells in surgical patients with non-small cell lung cancer: Does surgical manipulation dislodge cancer cells thus allowing them to pass into the peripheral blood? *Surg. Today* **46**, 1402–1409 (2016).
19. C. C. Sharkey, J. Li, S. Roy, Q. Wu, M. R. King, Two-stage nanoparticle delivery of piperlongumine and tumor necrosis factor-related apoptosis-inducing ligand (TRAIL) anti-cancer therapy. *Technology* **4**, 60–69 (2016).
20. X. Yang, Z. Li, Q. Wu, S. Chen, C. Yi, C. Gong, TRAIL and curcumin codelivery nanoparticles enhance TRAIL-induced apoptosis through upregulation of death receptors. *Drug Deliv.* **24**, 1526–1536 (2017).
21. K. Rana, C. A. Reinhart-King, M. R. King, Inducing apoptosis in rolling cancer cells: A combined therapy with aspirin and immobilized TRAIL and E-selectin. *Mol. Pharm.* **9**, 2219–2227 (2012).
22. M. J. Mitchell, M. R. King, Computational and experimental models of cancer cell response to fluid shear stress. *Front. Oncol.* **3**, 44 (2013).
23. F. Michor, J. Liphardt, M. Ferrari, J. Widom, What does physics have to do with cancer? *Nat. Rev. Cancer* **11**, 657–670 (2011).
24. M. Barrios, A. Rodríguez–Acosta, A. Gil, A. M. Salazar, P. Taylor, E. E. Sánchez, C. L. Arocha–Piñango, B. Guerrero, Comparative hemostatic parameters in BALB/c, C57BL/6 and C3H/He mice. *Thromb. Res.* **124**, 338–343 (2009).
25. J. A. Nemzek, G. L. Bolgos, B. A. Williams, D. G. Remick, Differences in normal values for murine white blood cell counts and other hematological parameters based on sampling site. *Inflamm. Res.* **50**, 523–527 (2001).
26. A. M. Brewster, M. Chavez-MacGregor, P. Brown, Epidemiology, biology, and treatment of triple-negative breast cancer in women of African ancestry. *Lancet Oncol.* **15**, e625–e634 (2014).
27. V. Masoud, G. Pagès, Targeted therapies in breast cancer: New challenges to fight against resistance. *World J. Clin. Oncol.* **8**, 120–134 (2017).
28. M. J. Mitchell, C. S. Chen, V. Ponmudi, A. D. Hughes, M. R. King, E-selectin liposomal and nanotube-targeted delivery of doxorubicin to circulating tumor cells. *J. Control. Release* **160**, 609–617 (2012).
29. W. D. Foulkes, I. M. Stefansson, P. O. Chappuis, L. R. Bégin, J. R. Goffin, N. Wong, M. Trudel, L. A. Akslen, Germline BRCA1 mutations and a basal epithelial phenotype in breast cancer. *J. Natl. Cancer Inst.* **95**, 1482–1485 (2003).
30. P. García-Teijido, M. L. Cabal, I. P. Fernández, Y. F. Pérez, Tumor-infiltrating lymphocytes in triple negative breast cancer: The future of immune targeting. *Clin. Med. Insights Oncol.* **10**, 31–39 (2016).
31. B. Vogelstein, N. Papadopoulos, V. E. Velculescu, S. Zhou, L. A. Diaz Jr., K. W. Kinzler, Cancer genome landscapes. *Science* **339**, 1546–1558 (2013).
32. S. Al-Mahmood, J. Sapiezynski, O. B. Garbuzenko, T. Minko, Metastatic and triple-negative breast cancer: Challenges and treatment options. *Drug Deliv. Transl. Res.* **8**, 1483–1507 (2018).
33. M. N. Dickler, M. A. Cobleigh, K. D. Miller, P. M. Klein, E. P. Winer, Efficacy and safety of erlotinib in patients with locally advanced or metastatic breast cancer. *Breast Cancer Res. Treat.* **115**, 115–121 (2009).
34. B. Thapa, R. Bahadur KC, H. Uludağ, Novel targets for sensitizing breast cancer cells to TRAIL-induced apoptosis with siRNA delivery. *Int. J. Cancer* **142**, 597–606 (2018).
35. X. Zhu, W. Zhou, The emerging regulation of VEGFR-2 in triple-negative breast cancer. *Front. Endocrinol.* **6**, 159 (2015).
36. R. Saraei, M. Soleimani, A. A. Movassaghpour Akbari, M. Farshdousti Hagh, A. Hassanzadeh, S. Solali, The role of XIAP in resistance to TNF-related apoptosis-inducing ligand (TRAIL) in leukemia. *Biomed. Pharmacother.* **107**, 1010–1019 (2018).
37. D. J. Taylor, C. E. Parsons, H. Han, A. Jayaraman, K. Rege, Parallel screening of FDA-approved antineoplastic drugs for identifying sensitizers of TRAIL-induced apoptosis in cancer cells. *BMC Cancer* **11**, 470 (2011).
38. A. Dréan, C. J. Lord, A. Ashworth, PARP inhibitor combination therapy. *Crit. Rev. Oncol. Hematol.* **108**, 73–85 (2016).
39. Q. Liu, Q. Tan, Y. Zheng, K. Chen, C. Qian, N. Li, Q. Wang, X. Cao, Blockade of Fas signaling in breast cancer cells suppresses tumor growth and metastasis via disruption of Fas signaling-initiated cancer-related inflammation. *J. Biol. Chem.* **289**, 11522–11535 (2014).
40. M. J. Mitchell, M. R. King, Fluid shear stress sensitizes cancer cells to receptor-mediated apoptosis via trimeric death receptors. *New J. Phys.* **15**, 015008 (2013).


**Acknowledgments:** We thank D. Liu for help in establishing the 4T1 mouse model, the Translational Pathology Shared Resource (TPSR) at the Vanderbilt University Medical Center for aid in specimen preparation for histology, and the animal care facility of Vanderbilt University. **Funding:** This work was supported by NIH grant no. R01 CA203991 to M.R.K. The Translational Pathology Shared Resource was supported by NCI/NIH Cancer Center Support Grant 5P30 CA68485-19 and the Vanderbilt Mouse Metabolic Phenotyping Center Grant 2 U24 DK059637-16. **Author contributions:** N.J. designed and performed the research, analyzed the data, and wrote the manuscript; Z.Z. prepared NL and ETL formulations; L.E.H. designed and carried out analysis of the in vivo toxicity studies; F.Y. helped with mice work; and M.R.K. conceived and supervised the research and edited the manuscript. **Competing interests:** The research described in this paper is related to U.S. Patent Application no. 14/909,523, entitled "Method to functionalize cells in human blood, other fluids and tissues using nanoparticles," on which M.R.K. is a coinventor, filed on 4 August 2014 by Cornell University. All other authors declare that they have no competing interests. **Data and materials availability:** All data needed to evaluate the conclusions in the paper are present in the paper and/or the Supplementary Materials. Additional data related to this paper may be requested from the authors.

Submitted 18 December 2018
Accepted 17 June 2019
Published 24 July 2019
10.1126/sciadv.aaw4197

**Citation:** N. Jyotsana, Z. Zhang, L. E. Himmel, F. Yu, M. R. King, Minimal dosing of leukocyte targeting TRAIL decreases triple-negative breast cancer metastasis following tumor resection. *Sci. Adv.* **5**, eaaw4197 (2019).

# Minimal dosing of leukocyte targeting TRAIL decreases triple-negative breast cancer metastasis following tumor resection

Nidhi Jyotsana, Zhenjiang Zhang, Lauren E. Himmel, Fang Yu and Michael R. King

*Sci Adv* **5** (7), eaaw4197.
DOI: 10.1126/sciadv.aaw4197